

# Task-Oriented Communication for Multi-Device Cooperative Edge Inference

Jiawei Shao, *Student Member, IEEE*, Yuyi Mao, *Member, IEEE*,  
and Jun Zhang, *Senior Member, IEEE*

## Abstract

This paper investigates task-oriented communication for multi-device cooperative edge inference, where a group of distributed low-end edge devices transmit the extracted features of local samples to a powerful edge server for inference. While cooperative edge inference can overcome the limited sensing capability of a single device, it substantially increases the communication overhead and may incur excessive latency. To enable low-latency cooperative inference, we propose a learning-based communication scheme that optimizes local feature extraction and distributed feature encoding in a task-oriented manner, i.e., to remove data redundancy and transmit information that is essential for the downstream inference task rather than reconstructing the data samples at the edge server. Specifically, we leverage an information bottleneck (IB) principle to extract the task-relevant feature at each edge device and adopt a distributed information bottleneck (DIB) framework to formalize a single-letter characterization of the optimal rate-relevance tradeoff for distributed feature encoding. To admit flexible control of the communication overhead, we extend the DIB framework to a distributed deterministic information bottleneck (DDIB) objective that explicitly incorporates the representational costs of the encoded features. As the IB-based objectives are computationally prohibitive for high-dimensional data, we adopt variational approximations to make the optimization problems tractable. To compensate the potential performance loss due to the variational approximations, we also develop a selective retransmission (SR) mechanism to identify the redundancy in the encoded features of multiple edge devices to attain additional communication overhead reduction. Extensive experiments evidence that the proposed task-oriented communication scheme achieves a better rate-relevance tradeoff than baseline methods.

The authors are with the Department of Electronic and Information Engineering, Hong Kong Polytechnic University, Hong Kong (E-mail: jiawei.shao@connect.polyu.hk, {yuyi-eie.mao, jun-eie.zhang}@polyu.edu.hk). (The corresponding author is J. Zhang.)

## Index Terms

Task-oriented communication, information bottleneck (IB), distributed information bottleneck (DIB), variational inference.

## I. INTRODUCTION

The recent revival of artificial intelligence (AI) has affected a plethora of application domains, including computer vision [1], augmented/virtual reality (AR/VR) [2], and natural language processing (NLP) [3]. Most recently, as edge devices (e.g., mobile phones, sensors) are becoming increasingly widespread and sensory data are easy to access, the potential of AI technologies has been exemplified at the network edge, which is a new research area named *edge inference* [4], [5]. Typical edge inference systems convey all the input data from the edge devices to a physically close edge server (e.g., a base station) and leverage deep neural networks (DNNs) to perform inference. However, as the volume of the collected data (e.g., images, high-definition videos, and point clouds) is enormous in typical mobile intelligent applications [6], [7], [8], directly transmitting the raw data to the edge server may lead to a prohibitive communication overhead.

To enable low-latency inference, *device-edge co-inference* stands out as a promising solution [9], [10], [11], which extracts task-relevant features from the raw input data and forwards them to be processed by an edge server. This exemplifies a recent shift in communication system design for emerging mobile applications, named *task-oriented communication*, which optimizes communication strategies for the downstream task [12]. While device-edge co-inference, together with task-oriented communication, has enabled low-latency inference for resource-constrained devices, its performance is limited by the sensing capability of a single device. In many applications, e.g., smart drones [7], robotics [8], and security camera systems [13], cooperative inference among multiple devices can significantly enhance the inference performance. Nevertheless, the communication overhead and latency may also increase substantially with the number of devices, forming the bottleneck for multi-device cooperative edge inference. Although most existing works on task-oriented communication have led to efficient communication for single-device edge inference, simply reusing these methods for multi-device cooperative edge inference is infeasible. This is because the correlation among the extracted features of different devices cannot be effectively exploited, which leads to excessive redundancy and latency in transmission. To address this limitation, this paper will develop task-oriented communication strategies for

multi-device cooperative edge inference by leveraging the information bottleneck (IB) principle proposed in [14], as well as the distributed information bottleneck (DIB) framework derived from distributed source coding theories [15], [16].

#### A. Related Works and Motivations

The recent line of research on task-oriented communication [17], [18] has motivated a paradigm shift in the communication system design. The conventional *data-oriented communication* aims to guarantee the correct reception of every single transmitted bit. However, with the increasing number of edge devices, the limited communication resources at the wireless network edge cannot cope with the request to transmit the huge volume of data. The task-oriented communication provides an alternative scheme to handle this challenge, which regards a part of the raw input data (e.g., nuisance) as irrelevant and considers to extract and transmit the task-relevant feature that could influence the inference result. As recovering the original input data with high fidelity at the edge server is unnecessary, task-oriented communication schemes leave abundant room for communication overhead reduction. This insight is consistent with the information bottleneck (IB) principle [14]: A good extracted feature should be *sufficient* for the inference task while retaining *minimal* information from the input data. Thus, extracting a *minimal sufficient feature* in task-oriented communication improves the transmission efficiency.

Recently, there exist several studies taking advantage of deep learning to develop effective feature extraction and encoding methods following the task-oriented design principle [19], [20], [12]. In particular, for the image classification task, an end-to-end architecture was proposed in [19] that leverages a JPEG compressor to encode the internal features. In contrast to data-oriented communication that concerns the data recovery quality, the proposed method is directly trained with the cross-entropy loss for the targeted classification task. Similar ideas were utilized in the image retrieval task [21] and the point cloud processing application [11]. Besides, the authors of [20] characterized the minimum bit rate of the extracted features required to ensure satisfactory performance of the predictive tasks. These features are learned from the unsupervised neural compressors that bound the encoded rates. Although the aforementioned works can largely reduce the communication overhead in single-device edge inference, simply extending them to the multi-device scenario is not efficient as their coding schemes cannot fully exploit the correlation among the extracted features of different devices, which necessitates the investigation of distributed feature encoding.

Distributed coding is an important problem in information theory and communication, which regards the data encoding of multiple correlated sources from different devices that do not communicate with each other. Remarkably, the Slepian-Wolf theorem [22] showed that the distributed coding rate is asymptotically equal to the joint coding rate. In other words, the redundancy among the dependent sources can be identified and eliminated in transmission. This classic result has recently received renewed attention and led to several works [23], [24], [25] to develop DNN-based distributed feature encoding schemes in task-oriented communication. The authors of [23] developed an optimal distributed quantization system tailored to the classification task, and proposed a greedy search algorithm as part of the deep learning approach to create rectangular quantization regions. Besides, a significance-aware feature selection mechanism was proposed in [24], which leverages a DNN model to determine the significance value of each feature and communicates only the features that are likely to impact the inference result. These methods have shown effectiveness in saving communication bandwidth compared with the single-device edge inference. However, there lacks a theoretical and rigorous way to characterize the tradeoff between the communication cost and the inference performance in distributed feature encoding, hindering further performance enhancement.

Recently, the distributed information bottleneck (DIB) framework [16] has been applied to investigate multi-view learning, which establishes a single-letter characterization of the optimal tradeoff between the rate (or representational cost) and relevance (or task-relevant information) for a class of memoryless sources using mutual information terms. Such an information-theoretical principle fits nicely with the multi-device cooperative edge inference. Thus, we leverage the IB principle [14] for task-relevant feature extraction and the DIB framework [16] to develop communication-efficient cooperative edge inference via optimizing the rate-relevance tradeoff. This demands additional optimizations to tackle the intractable mutual information terms, which is extremely challenging given the high-dimension data. Besides, as the optimal rate-relevance tradeoff obtained by the DIB framework is only satisfied in the asymptotic limit, practical feature encoding schemes should take the finite-block effect into consideration. These critical aspects form the main technical contributions of our study.

## *B. Contributions*

In this paper, we develop effective task-oriented communication schemes for multi-device cooperative edge inference. Our major contributions are summarized as follows:

- We formulate two design problems for task-oriented communication in multi-device cooperative edge inference systems, namely task-relevant feature extraction and distributed feature encoding. Specifically, we leverage the IB principle to design the task-relevant feature extraction at each edge device, which aims at extracting the minimum sufficient feature for the raw input data. Besides, the DIB framework is adopted to formalize a single-letter characterization of the optimal rate-relevance tradeoff in the distributed feature encoding, which is reformulated as the distributed deterministic information bottleneck (DDIB) objective to incorporate the representational costs of the encoded features.
- Observing that the mutual information terms in the IB-based objectives are computationally prohibitive for high-dimensional data, we resort to the variational approximations to devise the tractable upper bounds for the IB and DDIB objectives, resulting in the variational information bottleneck (VIB) objective and the variational distributed deterministic information bottleneck (VDDIB) objective, respectively.
- To compensate the potential performance loss due to the variational approximations, we introduce a selective retransmission (SR) mechanism in the VDDIB framework to identify the redundancy among the encoded features, which helps to further reduce the communication load. It also provides a flexible way to trade off the communication overhead with the inference performance.
- The effectiveness of the proposed task-oriented communication strategies is validated on a multi-view image classification task and a multi-view shape recognition task, which demonstrates a substantial reduction in the communication overhead compared with the traditional data-oriented communication strategy. Moreover, extensive simulation results demonstrate that our methods outperform existing learning-based feature encoding methods for cooperative inference.

### *C. Organization*

The rest of this paper is organized as follows. Section II introduces the system model and formulates the problems of task-relevant feature extraction and distributed feature encoding based on the IB and DIB frameworks, respectively. Section III proposes the VIB objective as a variational upper bound of the IB formulation for tractable optimization. Section IV reformulates the DIB objective to the DDIB objective and derives a tractable VDDIB objective for optimization of the distributed feature encoding. A selective retransmission mechanism is developed in Section

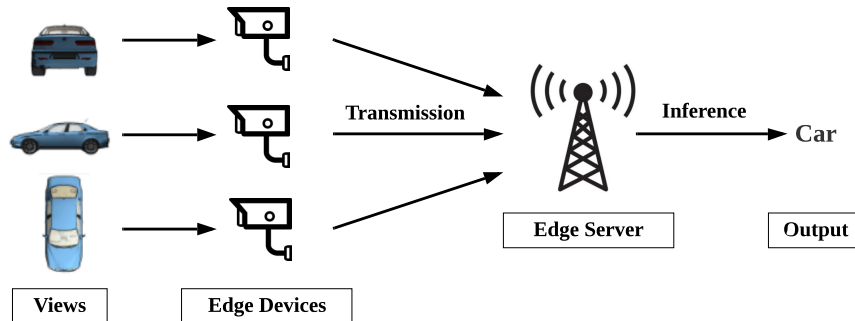


Fig. 1: An example of multi-device cooperative edge inference for multi-view shape recognition.

V to further reduce the communication overhead. In Section VI, we provide extensive simulation results to evaluate the performance of the proposed methods. Finally, Section VII concludes the paper.

#### D. Notations

Throughout this paper, upper-case letters (e.g.  $X, Y$ ) and lower-case letters (e.g.  $\mathbf{x}, \mathbf{y}$ ) stand for random variables and their realizations, respectively. We use  $X_{1:K}$  to represent the set of random variables  $(X_1, \dots, X_K)$ . The entropy of  $Y$  and the conditional entropy of  $Y$  given  $X$  are denoted as  $H(Y)$  and  $H(Y|X)$ , respectively. The mutual information between  $X$  and  $Y$  is represented as  $I(X, Y)$ , and the Kullback-Leibler (KL) divergence between two probability distributions  $p(\mathbf{x})$  and  $q(\mathbf{x})$  is denoted as  $D_{\text{KL}}(p||q)$ . The statistical expectation of  $X$  is denoted as  $\mathbf{E}(X)$ . We further denote the Gaussian distribution with mean vector  $\boldsymbol{\mu}$  and covariance matrix  $\boldsymbol{\Sigma}$  as  $\mathcal{N}(\boldsymbol{\mu}, \boldsymbol{\Sigma})$ , and use  $\mathbf{I}$  to represent the identity matrix. The element-wise product is denoted as  $\odot$ .

## II. SYSTEM MODEL AND PROBLEM DESCRIPTION

We consider a multi-device cooperative edge inference system, where a group of low-end edge devices collaborate to perform an inference task with the assistance of an edge server. These devices perceive different views of the same object, and therefore cooperative inference can effectively overcome the limited sensing capability of a single device [26]. Related application scenarios include multi-view object detection [26] in security camera systems and vehicle re-identification [13] in urban surveillance. A sample system for multi-view shape recognition is shown in Fig. 1. Compared with the edge devices, the edge server has abundant computational

resources so that server-based inference can be executed in real time by collecting the sensing data from multiple edge devices. Nevertheless, edge inference systems typically suffer from limited communication bandwidth, and thus directly transmitting the raw sensory data (e.g., high-definition images and point clouds) from the edge devices to the edge server shall incur significant communication latency. To enable low-latency cooperative edge inference, it is critical to design efficient task-oriented communication strategies that only transmit the task-relevant information to the edge server for device-edge co-inference. Next, we first present a probabilistic modeling of the multi-device cooperative edge inference systems and introduce two key design problems of task-oriented communication, namely, task-relevant feature extraction and distributed feature encoding.

### A. Probabilistic Modeling

The probabilistic modeling for multi-device cooperative edge inference, comprising  $K$  edge devices and an edge server, is shown in Fig. 2. The input views of different edge devices, denoted as  $(\mathbf{x}_1, \dots, \mathbf{x}_K)$ , and the target variable  $\mathbf{y}$  (e.g., the category of an object), are deemed as different realizations of the random variables  $(X_1, \dots, X_K, Y)$  with joint distribution  $p(\mathbf{x}_1, \dots, \mathbf{x}_K, \mathbf{y})$ . To perform cooperative inference, each edge device first extracts the task-relevant feature  $\mathbf{z}_k$  from the input  $\mathbf{x}_k$ , and encodes the extracted feature to a compact vector  $\mathbf{u}_k$  for efficient transmission to the edge server. After receiving the encoded features from the edge devices, the edge server performs further processing to derive the final inference result. The extracted features  $(\mathbf{z}_1, \dots, \mathbf{z}_K)$  and the encoded features  $(\mathbf{u}_1, \dots, \mathbf{u}_K)$  are instantiated by random variables  $(Z_1, \dots, Z_K)$  and  $(U_1, \dots, U_K)$ , respectively. These random variables constitute the following Markov chain:

$$Y \leftrightarrow X_k \leftrightarrow Z_k \leftrightarrow U_k, \quad \forall k \in \{1, \dots, K\}, \quad (1)$$

which satisfies  $p(\mathbf{u}_k, \mathbf{z}_k, \mathbf{x}_k | \mathbf{y}) = p(\mathbf{u}_k | \mathbf{z}_k) p(\mathbf{z}_k | \mathbf{x}_k) p(\mathbf{x}_k | \mathbf{y})$ ,  $\forall k \in \{1, \dots, K\}$ . A key design objective is to minimize the communication overhead while providing satisfactory inference performance. The proposed solution involves effective local feature extraction and distributed feature encoding, which are specified in the following two subsections.

### B. Task-Relevant Feature Extraction

Given the high dimension of the sensing data, a significant part of the input  $X_k$  at the  $k$ -th device is superfluous to the target variable  $Y$ . To achieve efficient task-oriented communication, the

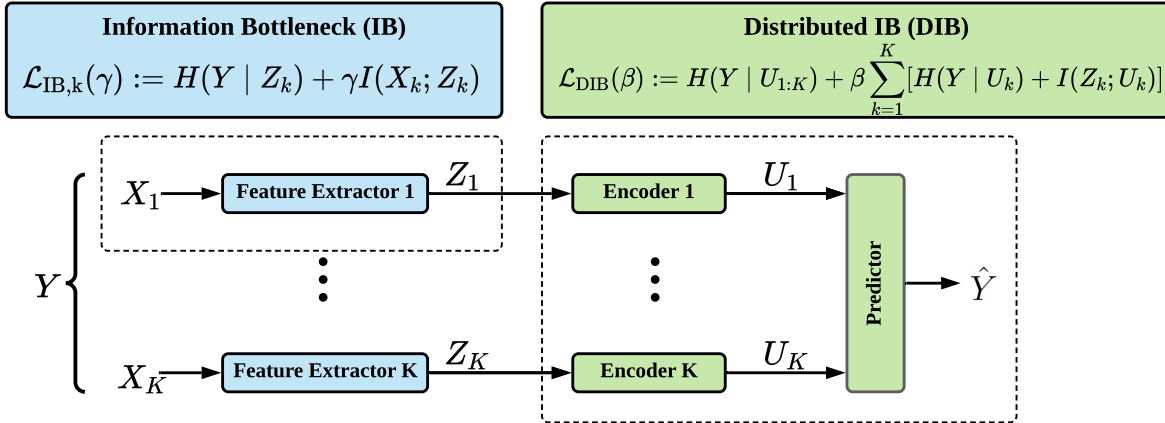


Fig. 2: Probabilistic modeling for multi-device cooperative edge inference systems.

extracted feature  $Z_k$  should capture only the task-relevant information about the target variable  $Y$  from the observation  $X_k$ . Our design follows the information bottleneck (IB) principle [14], which was shown to be effective for feature extraction and encoding in single-device edge inference systems [12]. The core idea of the IB framework is to extract a *minimal sufficient* feature  $Z_k$  from  $X_k$ , which should contain sufficient information related to  $Y$ , while retaining minimal information about  $X_k$ . These notions can be nicely characterized via information-theoretic measures [14], [27]. In particular, minimality means  $I(X_k; Z_k) \leq I(Y; X_k)$  since any information related to  $X_k$  but unrelated to  $Y$  is redundant; Sufficiency implies  $I(Y; Z_k) \geq I(Y; X_k)$ , where  $Z_k$  should be at least as informative as  $X_k$  for predicting  $Y$ . By further incorporating the data processing inequality, i.e.,  $I(Y; Z_k) \leq I(X_k; Z_k)$ , a minimal sufficient feature  $Z_k$  should satisfy the following criteria:

$$\underbrace{I(X_k; Z_k)}_{\text{Minimality}} = \overbrace{I(Y; X_k) = I(Y; Z_k)}^{\text{Sufficiency}}, \quad k \in \{1, \dots, K\}. \quad (2)$$

Thus, to devise a feature  $Z_k$  that satisfies (2), we minimize the weighted sum of  $-I(Y; Z_k)$  and  $I(X_k; Z_k)$  via the following IB objective:

$$\mathcal{L}_{\text{IB},k}(\gamma) := H(Y|Z_k) + \gamma I(X_k; Z_k), \quad (3)$$

where  $\gamma \geq 0$  is a weighting factor and the constant term  $H(Y)$  is eliminated as  $I(Y; Z_k) = H(Y) - H(Y|Z_k)$ . However, minimizing the IB objective function in (3) requires to compute the marginal distribution of  $Z_k$ , which is expensive especially for the high-dimensional variables.

To tackle this issue, we resort to the variational method to reformulate (3) into a computationally amenable form in Section III.

### C. Distributed Feature Encoding

Once the task-relevant feature is extracted, it will be encoded for efficient transmission. Intuitively, there is an implicit tradeoff between rate and relevance: The inference accuracy can be improved by transmitting more task-relevant information from multiple edge devices at the cost of increased communication overhead. By analogy with the rate-distortion tradeoff in source coding problems [15], [28], we characterize the *rate-relevance* tradeoff in edge inference. Consider a feature encoding scheme with blocklength  $N$ , which maps the extracted features  $Z_k^{1:N} = (Z_k^1, \dots, Z_k^N)$  of  $N$  input samples to a codeword that belongs to set  $\mathcal{M}_k^N$ . The decoder at the edge server processes the codewords from devices to derive the inference result  $\hat{Y}^N$ . The relevance  $\Delta^N$  that measures the accuracy of the inference result  $\hat{Y}^N$  and the rate  $R_k^N$  accounting for the communication overhead of edge device  $k$  are defined respectively as follows:

$$\Delta^N := \frac{1}{N} I(Y^N; \hat{Y}^N), \quad (4)$$

$$R_k^N \geq \frac{1}{N} \log |\mathcal{M}_k^N|, \quad k \in \{1, \dots, K\}. \quad (5)$$

We endeavor to develop a set of distributed feature encoders for the edge devices and a joint decoder for the edge server that maximize the relevance while reducing the sum of the communication costs, i.e.,  $R_{\text{sum}}^N := \sum_{k=1}^K R_k^N$ . The performance of the multi-device cooperative edge inference system can be characterized by the achievable rate-relevance region, as specified in the following definition.

**Definition 1.** A tuple  $(\Delta, R_{\text{sum}})$  is said to be achievable if there exists a blocklength- $N$  feature encoding scheme that satisfies the following inequalities:

$$\Delta \leq \Delta^N \quad \text{and} \quad R_{\text{sum}} \geq R_{\text{sum}}^N. \quad (6)$$

The rate-relevance region is given by the closure of all the achievable  $(\Delta, R_{\text{sum}})$  tuples.

The following proposition establishes a single-letter characterization of the optimal rate-relevance tuples in multi-device cooperative edge inference systems.

**Proposition 1.** *Suppose the extracted features satisfy the minimality condition in (2). Each  $(\Delta_\beta, R_\beta)$  with  $\beta \geq 0$  is an optimal rate-relevance tuple, i.e., there exists no relevance  $\Delta \geq \Delta_\beta$  given the sum rate constraint  $R_{\text{sum}} = R_\beta$ , where*

$$\Delta_\beta = I(Y; U_{1:K}^*), \quad (7)$$

$$R_\beta = \Delta_\beta + \sum_{k=1}^K [I(Z_k; U_k^*) - I(Y; U_k^*)], \quad (8)$$

and the encoded features  $U_{1:K}^*$  are obtained by minimizing the following distributed information bottleneck (DIB) objective:

$$\min_{\{p(\mathbf{u}_k|\mathbf{z}_k)\}_{k=1}^K} \mathcal{L}_{\text{DIB}}(\beta) := H(Y|U_{1:K}) + \beta \sum_{k=1}^K [H(Y|U_k) + I(Z_k; U_k)]. \quad (9)$$

*Proof.* The proof is given in Appendix A. □

Proposition 1 shows that the optimal distributed feature encoding scheme can be obtained by minimizing the DIB objective in (9), where the parameter  $\beta$  balances the communication overhead and inference performance. However, the optimal rate-relevance tuples are achievable only in the asymptotic limit when  $N$  approaches infinity. In other words, the edge inference system needs to accumulate a significant amount of input samples before performing distributed feature encoding, which shall postpone the inference process. To enable instantaneous edge inference for each input sample, we reformulate the DIB framework to a distributed deterministic information bottleneck (DDIB) objective in Section IV, which replaces mutual information terms  $I(Z_k; U_k)$  with the representational costs  $R_{\text{bit}}(U_k)$  (i.e., the number of bits) of the encoded features. Besides, we adopt variational approximations to derive an upper bound for the conditional entropy terms  $H(Y|U_{1:K})$  and  $\{H(Y|U_k)\}_{k=1}^K$  for more tractable optimization.

### III. VARIATIONAL APPROXIMATION FOR FEATURE EXTRACTION

In this section, we leverage a variational information bottleneck (VIB) framework to reformulate the IB objective derived in Section II-B to facilitate tractable optimization of feature extraction.

#### A. Variational Information Bottleneck

Recall the IB objective in (3) with the form of  $\mathcal{L}_{\text{IB},k}(\gamma) := H(Y|Z_k) + \gamma I(X_k; Z_k)$  for device  $k$ . Let  $p_{\theta_k}(\mathbf{z}_k|\mathbf{x}_k)$  denote the conditional distribution parameterized by  $\theta_k$  that represents the feature

extraction process. Given the joint distribution  $p(\mathbf{x}_k, \mathbf{y})$  and the Markov chain  $Y \leftrightarrow X_k \leftrightarrow Z_k$  in (1), the marginal distribution  $p(\mathbf{z}_k)$  and the conditional distribution  $p(\mathbf{y}|\mathbf{z})$  are fully determined by the conditional distribution  $p_{\theta_k}(\mathbf{z}_k|\mathbf{x}_k)$  as follows:

$$p(\mathbf{z}_k) = \int p(\mathbf{x}_k)p_{\theta_k}(\mathbf{z}_k|\mathbf{x}_k)d\mathbf{x}_k, \quad (10)$$

$$p(\mathbf{y}|\mathbf{z}_k) = \frac{\int p(\mathbf{x}_k, \mathbf{y})p_{\theta_k}(\mathbf{z}_k|\mathbf{x}_k)d\mathbf{x}_k}{p(\mathbf{z}_k)}. \quad (11)$$

However, the distributions  $p(\mathbf{z}_k)$  and  $p(\mathbf{y}|\mathbf{z}_k)$  are generally intractable due to the high dimensionality. Similar to [12], we adopt tools from variational inference to approximate these intractable distributions. The idea of the variational approximation is to posit a family of distributions and find a member of that family which is close to the target distribution [29]. Specifically, we introduce  $r_k(\mathbf{z}_k)$  and  $p_{\varphi_k}(\mathbf{y}|\mathbf{z}_k)$  as the variational distributions to approximate  $p(\mathbf{z}_k)$  and  $p(\mathbf{y}|\mathbf{z}_k)$ , respectively. The family of variational conditional distributions is parameterized by  $\varphi_k$ . With the aid of these approximations, we derive a VIB objective as an upper bound of the IB objective as follows:

$$\mathcal{L}_{\text{VIB},k}(\gamma; \boldsymbol{\theta}_k, \boldsymbol{\varphi}_k) = \mathbf{E}_{p(\mathbf{x}_k, \mathbf{y})} \left\{ \mathbf{E}_{p_{\theta_k}(\mathbf{z}_k|\mathbf{x}_k)} [-\log p_{\varphi_k}(\mathbf{y}|\mathbf{z}_k)] + \gamma D_{\text{KL}}(p_{\theta_k}(\mathbf{z}_k|\mathbf{x}_k) || r_k(\mathbf{z}_k)) \right\}, \quad (12)$$

for which, the detailed derivation is available in Appendix B-A.

### B. DNN Parameterization

To take advantage of deep learning, we formulate the distributions  $p_{\theta_k}(\mathbf{z}_k|\mathbf{x}_k)$  and  $p_{\varphi_k}(\mathbf{y}|\mathbf{z}_k)$  in terms of DNNs with parameters  $\boldsymbol{\theta}_k, \boldsymbol{\varphi}_k$ . A common approach to parameterize the condition distribution  $p_{\theta_k}(\mathbf{z}_k|\mathbf{x}_k)$  is adopting the multivariate Gaussian distribution [27], i.e.,  $p_{\theta_k}(\mathbf{z}_k|\mathbf{x}_k) = \mathcal{N}(\mathbf{z}_k|\boldsymbol{\mu}_k, \boldsymbol{\Sigma}_k)$ , where the mean vector  $\boldsymbol{\mu}_k = (\mu_{k,1}, \dots, \mu_{k,d}) \in \mathbb{R}^d$  is determined by the DNN-based function  $\boldsymbol{\mu}_k(\mathbf{x}_k; \boldsymbol{\theta}_k)$  parameterized by  $\boldsymbol{\theta}_k$ , and the covariance matrix  $\boldsymbol{\Sigma}_k$  is represented by a diagonal matrix  $\text{diag}\{\sigma_{k,1}^2, \dots, \sigma_{k,d}^2\}$  with  $\boldsymbol{\sigma}_k = (\sigma_{k,1}, \dots, \sigma_{k,d}) \in \mathbb{R}^d$  determined by the DNN-based function  $\boldsymbol{\sigma}_k(\mathbf{x}_k; \boldsymbol{\theta}_k)$ . Besides, the variational marginal distribution  $r_k(\mathbf{z}_k)$  is approximated as a centered isotropic Gaussian distribution  $\mathcal{N}(\mathbf{z}_k|\mathbf{0}, \mathbf{I})$ . As a result, we simplify the KL-divergence term in (12) as follows:

$$D_{\text{KL}}(p_{\theta_k}(\mathbf{z}_k|\mathbf{x}_k) || r_k(\mathbf{z}_k)) = \sum_{i=1}^d \left\{ \frac{\mu_{k,i}^2 + \sigma_{k,i}^2 - 1}{2} - \log \sigma_{k,i} \right\}. \quad (13)$$

---

**Algorithm 1** Training Procedures for the Task-Relevant Feature Extraction at Device  $k$ 


---

**Input:** Training dataset  $\mathcal{D}$ , batch size  $M$ , initialized parameters  $\theta_k, \varphi_k$ .

**Output:** The optimized parameters  $\theta_k$  and  $\varphi_k$

- 1: **repeat**
  - 2:   Randomly select a minibatch of data  $\{(\mathbf{x}_k^m, \mathbf{y}^m)\}_{m=1}^M$  from  $\mathcal{D}$ .
  - 3:   Compute the mean vector  $\{\boldsymbol{\mu}_k^m\}_{m=1}^M$  and the standard deviation vector  $\{\boldsymbol{\sigma}_k^m\}_{m=1}^M$ .
  - 4:   **while**  $m = 1$  to  $M$  **do**
  - 5:     Sample  $\boldsymbol{\epsilon}_k^m \sim \mathcal{N}(\mathbf{0}, \mathbf{I})$ .
  - 6:     Compute  $\mathbf{z}_k^m = \boldsymbol{\mu}_k^m + \boldsymbol{\sigma}_k^m \odot \boldsymbol{\epsilon}_k^m$ .
  - 7:   **end while**
  - 8:   Compute the loss  $\mathcal{L}_{\text{VIB},k}(\gamma; \theta_k, \varphi_k)$  based on (14).
  - 9:   Update parameters  $\theta_k, \varphi_k$  through backpropagation.
  - 10: **until** Convergence of parameters  $\theta_k$  and  $\varphi_k$
- 

To optimize the negative log-likelihood term in (12), we adopt the reparameterization trick [30] to sample  $\mathbf{z}_k$  from the learned distribution  $p_{\theta_k}(\mathbf{z}_k|\mathbf{x}_k)$ , where  $\mathbf{z}_k = \boldsymbol{\mu}_k + \boldsymbol{\sigma}_k \odot \boldsymbol{\epsilon}_k$ , and  $\boldsymbol{\epsilon}_k$  is sampled from  $\mathcal{N}(\mathbf{0}, \mathbf{I})$ . In this case, the Monte Carlo estimate of the negative log-likelihood term is differentiable with respect to  $\theta_k$ . The inference result is obtained based on the extracted feature  $\mathbf{z}_k$  by the function  $\hat{\mathbf{y}}(\mathbf{z}_k; \varphi_k)$  with parameters  $\varphi_k$ . We formulate the variational conditional distribution as  $p_{\varphi_k}(\mathbf{y}|\mathbf{z}_k) \propto \exp(-\ell(\mathbf{y}_k, \hat{\mathbf{y}}(\mathbf{z}_k; \varphi_k)))$ , where  $\ell(\cdot, \cdot)$  denotes the loss function to measure the discrepancy between  $\mathbf{y}$  and  $\hat{\mathbf{y}}_k$ . By applying the Monte Carlo sampling method, we obtain an unbiased estimate of the gradient and hence optimize the objective function in (12). In particular, given a minibatch of data  $\{(\mathbf{x}_k^m, \mathbf{y}^m)\}_{m=1}^M$  at device  $k$ , we have the following empirical estimation of the VIB objective:

$$\mathcal{L}_{\text{VIB},k}(\gamma; \theta_k, \varphi_k) \simeq \frac{1}{M} \sum_{m=1}^M \{-\log p_{\varphi_k}(\mathbf{y}^m|\mathbf{z}_k^m) + \gamma D_{\text{KL}}(p_{\theta_k}(\mathbf{z}_k^m|\mathbf{x}_k^m)||r_k(\mathbf{z}_k^m))\}. \quad (14)$$

The training procedures for task-relevant feature extraction are summarized in Algorithm 1.

#### IV. VARIATIONAL DISTRIBUTED FEATURE ENCODING

In this section, we develop a distributed feature encoding scheme based on the DIB objective in (9) to achieve efficient task-oriented communication. We first reformulate the DIB objective to a *distributed deterministic information bottleneck* (DDIB) objective that explicitly takes into account the communication overhead of each encoded feature. Besides, variational approximations are invoked again to make the optimization of the DDIB objective tractable.

### A. Distributed Deterministic Information Bottleneck Reformulation

The DIB objective in (9) measures the data rate by the mutual information terms  $I(Z_k, U_k)$  for  $k \in \{1, \dots, K\}$ . Although the mutual information has broad applications in representation learning [16], [31], directly controlling the amount of resources required to represent each  $U_k$  (i.e., the number of bits) is more relevant in communication systems. To address the communication cost, we select a deterministic encoding function that maps each task-relevant feature  $Z_k$  to a bitstream  $U_k$ , and adopt the number of bits, denoted as  $R_{\text{bit}}(U_k)$ , to measure the communication overhead, which results in the following DDIB objective:

$$\mathcal{L}_{\text{DDIB}}(\beta) := H(Y|U_{1:K}) + \beta \sum_{k=1}^K [H(Y|U_k) + R_{\text{bit}}(U_k)]. \quad (15)$$

In particular, the feature encoder in each edge device first performs the encoding transformation  $\mathbf{f}_{\phi_k}$ , followed by the quantization  $\mathcal{Q}_k$ , i.e., the encoded feature is given by  $\mathbf{u}_k = \mathcal{Q}_k(\mathbf{f}_{\phi_k}(z_k))$ . We select each  $\mathcal{Q}_k$  as a uniform quantizer that discretizes each element in  $\mathbf{f}_{\phi_k}(z_k) \in \mathbb{R}^{d_k}$  into  $n_k$  bits, and leverages the straight-through estimator (STE) [32] to approximate the gradients for backpropagation in the training process. In other words,  $R_{\text{bit}}(\mathbf{u}_k) = n_k d_k$  bits need to be transmitted in order to transfer the encoded feature  $\mathbf{u}_k$  from device  $k$  to the edge server<sup>1</sup>.

### B. Variational Distributed Deterministic Information Bottleneck

The conditional distributions  $\{p(\mathbf{y}|\mathbf{u}_k)\}_{k=1}^K$  and  $p(\mathbf{y}|\mathbf{u}_{1:K})$  are fully determined given deterministic mappings from  $Z_k$  to  $U_k$ ,  $k \in \{1, \dots, K\}$ . However, calculating the conditional entropy terms  $H(Y|U_{1:K})$  and  $H(Y|U_k)$  in (15) is generally intractable due to the high-dimensional integrals. Following Section III, we adopt variational distributions  $p_{\psi_0}(\mathbf{y}|\mathbf{u}_{1:K})$  and  $\{p_{\psi_k}(\mathbf{y}|\mathbf{u}_k)\}_{k=1}^K$  to replace the terms  $p(\mathbf{y}|\mathbf{u}_{1:K})$  and  $\{p(\mathbf{y}|\mathbf{u}_k)\}_{k=1}^K$ . By denoting  $\psi := \{\psi_0, \{\psi_k\}_{k=1}^K\}$  as the DNN parameters for the variational distributions, we derive a *variational distributed deterministic information bottleneck* (VDDIB) objective as follows:

$$\mathcal{L}_{\text{VDDIB}}(\beta; \phi, \psi) := \mathbf{E}_{p_{\theta}(z_{1:K}, \mathbf{y})} \left\{ -\log p_{\psi_0}(\mathbf{y}|\mathbf{u}_{1:K}) + \beta \left\{ \sum_{k=1}^K -\log p_{\psi_k}(\mathbf{y}|\mathbf{u}_k) + \sum_{k=1}^K R_{\text{bit}}(\mathbf{u}_k) \right\} \right\}, \quad (16)$$

<sup>1</sup>Note that the quantization scheme is orthogonal to the proposed DDIB method. The reason for selecting the uniform quantization in this paper is that we can easily approximate the gradients and calculate the bit-length.

---

**Algorithm 2** Training Procedures for the VDDIB Method
 

---

**Input:** Training dataset  $\mathcal{D}$ , batch size  $M$ , optimized parameters  $\{\theta_k\}_{k=1}^K$ , and initialized parameters  $\phi, \psi$ .

**Output:** The optimized parameters  $\phi$  and  $\psi$ .

1: **repeat**

2: Randomly select a minibatch of data  $\{(\mathbf{x}_{1:K}^m, \mathbf{y}^m)\}_{m=1}^M$  from  $\mathcal{D}$ .

3: Extract the task-relevant features  $\{\mathbf{z}_{1:K}^m\}_{m=1}^M$  based on the learned distributions  $\{p_{\theta_k}(\mathbf{z}_k|\mathbf{x}_k)\}_{k=1}^K$ .

4: Compute the loss  $\mathcal{L}_{\text{VDDIB}}(\beta; \phi, \psi)$  based on (19).

5: Update parameters  $\phi, \psi$  through backpropagation.

6: **until** Convergence of parameters  $\phi$  and  $\psi$ .

---

which is an upper bound of the DDIB objective as shown in Appendix B-B. The variational distributions are formulated as follows:

$$p_{\psi_0}(\mathbf{y}|\mathbf{u}_{1:K}) \propto \exp(-\ell(\mathbf{y}, \hat{\mathbf{y}}(\mathbf{u}_{1:K}; \psi_0))), \quad (17)$$

$$p_{\psi_k}(\mathbf{y}|\mathbf{u}_k) \propto \exp(-\ell(\mathbf{y}, \hat{\mathbf{y}}(\mathbf{u}_k; \psi_k))), k \in \{1, \dots, K\}, \quad (18)$$

where the functions  $\hat{\mathbf{y}}(\mathbf{u}_{1:K}; \psi_0)$  and  $\{\hat{\mathbf{y}}(\mathbf{u}_k; \psi_k)\}_{k=1}^K$  can be interpreted as the predictors that use the received features to predict the target variable. In the training process, by leveraging the Monte Carlo sampling method as in (14) and selecting a minibatch  $\{(\mathbf{z}_{1:K}^m, \mathbf{y}^m)\}_{m=1}^M$  from the joint distribution  $p_{\theta}(\mathbf{z}_{1:K}, \mathbf{y})$ , we have the following expression to estimate the VDDIB objective function:

$$\mathcal{L}_{\text{VDDIB}}(\beta; \phi, \psi) \simeq \frac{1}{M} \sum_{m=1}^M \left\{ -\log p_{\psi_0}(\mathbf{y}^m|\mathbf{u}_k^m) + \beta \sum_{k=1}^K \left\{ -\log p_{\psi_k}(\mathbf{y}^m|\mathbf{u}_k^m) + R_{\text{bit}}(\mathbf{u}_k^m) \right\} \right\}. \quad (19)$$

The joint distribution  $p_{\theta}(\mathbf{z}_{1:K}, \mathbf{y}) = \int p(\mathbf{x}_{1:K}, \mathbf{y}) \prod_{k=1}^K p_{\theta_k}(\mathbf{z}_k|\mathbf{x}_k) d\mathbf{x}_{1:K}$  with parameters  $\{\theta_k\}_{k=1}^K$  is obtained by the task-relevant feature extraction learned from Algorithm 1. The optimization procedures for the VDDIB objective are summarized in Algorithm 2.

**Remark 1.** *The VDDIB objective is an upper bound of the DIB objective as shown in the following expression, owing to  $I(Z_k, U_k) \leq H(U_k) \leq R_{\text{bit}}(U_k)$  and the variational approximations:*

$$\mathcal{L}_{\text{DIB}}(\beta) \leq \mathcal{L}_{\text{DDIB}}(\beta) \leq \mathcal{L}_{\text{VDDIB}}(\beta; \phi, \psi). \quad (20)$$

*It is important to note that the distributed feature encoding scheme obtained by minimizing the VDDIB objective does not guarantee to achieve the optimal rate-relevance tuples in Proposition 1 due to the approximations in the IB and DIB optimizations. Nevertheless, the empirical results in*

*Section VI-C evidence that the proposed method notably outperforms the existing communication strategies for multi-device cooperative edge inference.*

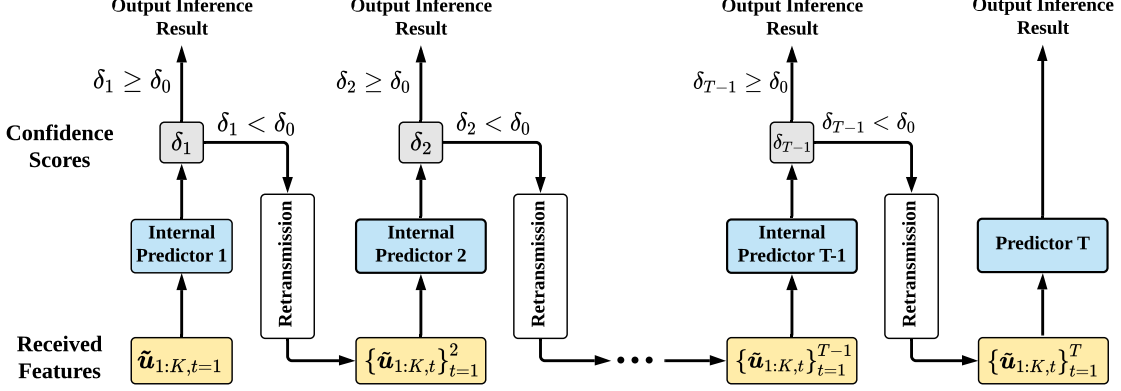
## V. DISTRIBUTED FEATURE ENCODING WITH SELECTIVE RETRANSMISSION

As highlighted in Remark 1, minimizing the VDDIB objective may not result in the optimal rate-relevance tuples. To further reduce the communication overhead, we need more effective approaches to identify the redundancy in the encoded features of multiple edge devices. For this purpose, we propose a VDDIB-SR method that introduces a *selective retransmission* (SR) mechanism to the VDDIB framework, where the edge server selectively activates the edge devices to retransmit their encoded features based on the informativeness of all the received features.

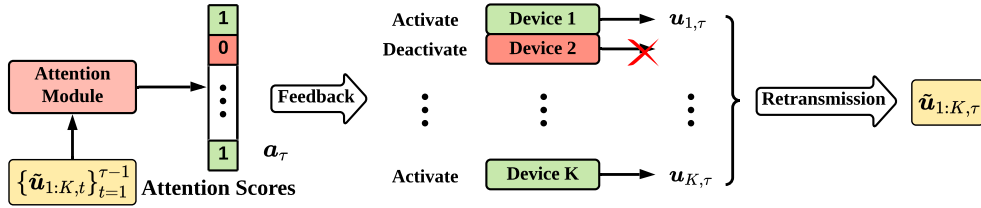
### A. Selective Retransmission Mechanism

We assume each edge device is allowed to transmit the encoded feature  $\{U_{k,t}\}_{t=1}^T$  with a maximum number of  $T$  attempts (i.e.,  $T - 1$  retransmissions), where  $U_k := \{U_{k,t}\}_{t=1}^T$ . The deterministic mapping from  $Z_k$  to  $U_k$  is defined as  $\{\mathbf{u}_{k,t}\}_{t=1}^T = \mathcal{Q}_k(\mathbf{f}_{\tilde{\phi}_k}(z_k))$ . The feature encoding transformation  $\mathbf{f}_{\tilde{\phi}_k}$  is a DNN-based function parameterized by  $\tilde{\phi}_k$ . All the parameters  $\{\tilde{\phi}_k\}_{k=1}^K$  are defined as  $\tilde{\phi}$  for simplicity. The edge server leverages the received features for inference after each transmission. Once the received features are sufficient to output a confident result, the remaining retransmission attempts can be saved, which is favorable for latency reduction. To unleash the full benefits of the selective retransmission mechanism, it is critical to design a *stopping polity* to decide when to terminate the retransmission process. Besides, as the encoded features of multiple edge devices may be redundant for edge inference, it leaves room for further communication overhead reduction by scheduling the edge devices with the most informative features for retransmissions. Thus, an *attention module* is proposed that activates the edge devices with the most informative features to retransmit. The received features from the activated devices in the  $t$ -th transmission are defined as  $\tilde{\mathbf{u}}_{1:K,t}$ .

1) *Stopping Policy*: Inspired by cascade inference [33], [34], we develop a confidence-based stopping policy at the edge server that outputs the confidence scores  $\delta_\tau$ ,  $\tau \in \{1, \dots, T - 1\}$ , of the inference results after each transmission attempt. Its structure is depicted in Fig. 3a, which consists of  $T - 1$  internal predictors, and the confidence scores determine when to terminate the



(a) The stopping policy that determines when to terminate the retransmission process.



(b) The attention module that determines which devices to retransmit.

Fig. 3: The selective retransmission mechanism with (a) a stopping policy and (b) an attention module.

retransmission process. Specifically, the  $\tau$ -th internal predictor outputs the inference result based on the received features  $\{\tilde{\mathbf{u}}_{1:K,t}\}_{t=1}^{\tau}$  defined as follows:

$$\textbf{Internal Predictors: } \hat{\mathbf{y}} \left( \{\tilde{\mathbf{u}}_{1:K,t}\}_{t=1}^{\tau}; \tilde{\boldsymbol{\psi}}_{\tau} \right), \tau \in \{1, \dots, T\}, \quad (21)$$

where  $\tilde{\boldsymbol{\psi}}_{\tau}$  represent the DNN parameters that form the  $\tau$ -th internal predictor, and we define  $\tilde{\boldsymbol{\psi}} := \{\tilde{\boldsymbol{\psi}}_t\}_{t=1}^T$  for notational simplicity. The corresponding variational distributions are as follows:

$$p_{\tilde{\boldsymbol{\psi}}_{\tau}}(\mathbf{y} | \{\tilde{\mathbf{u}}_{1:K,t}\}_{t=1}^{\tau}) \propto \exp \left( -\ell(\mathbf{y}, \hat{\mathbf{y}} \left( \{\tilde{\mathbf{u}}_{1:K,t}\}_{t=1}^{\tau}; \tilde{\boldsymbol{\psi}}_{\tau} \right)) \right), \tau \in \{1, \dots, T\}. \quad (22)$$

A threshold value  $\delta_0$  is selected to decide when to terminate the retransmission process: If a confidence score  $\delta_{\tau}$  is above  $\delta_0$ , the intermediate inference result is likely to be correct, and the inference process is terminated with that result; Otherwise, more features from the edge devices are preferred by the edge server to improve the inference performance. In other words, the threshold value  $\delta_0$  allows us to flexibly control the tradeoff between the inference performance and the communication overhead. Particularly, we use the maximum predicted probability as the confidence score for the classification tasks expressed as follows:

$$\textbf{Confidence Scores: } \delta_{\tau} = \max \left( \hat{\mathbf{y}} \left( \{\tilde{\mathbf{u}}_{1:K,t}\}_{t=1}^{\tau}; \tilde{\boldsymbol{\psi}}_{\tau} \right) \right), \tau \in \{1, \dots, T-1\}. \quad (23)$$

2) *Attention Module*: The attention module is developed to determine which devices should be activated for retransmissions. Each attention score  $a_{k,\tau} \in \{0, 1\}$  for the edge device  $k$  in the  $\tau$ -th transmission is based on the received features  $\{\tilde{\mathbf{u}}_{1:K,t}\}_{t=1}^{\tau-1}$  determined as follows:

$$\mathbf{Attention\ Scores:} \quad a_{k,\tau} = g_{k,\tau-1}(\{\tilde{\mathbf{u}}_{1:K,t}\}_{t=1}^{\tau-1}), \quad k \in \{1, \dots, K\} \text{ and } \tau \in \{2, \dots, T\}, \quad (24)$$

where functions  $\{g_{k,1}, \dots, g_{k,T-1}\}_{k=1}^K$  are constructed by fully-connected layers. Particularly, we set  $a_{k,1} = 1$ ,  $k \in \{1, \dots, K\}$ , which means that all the edge devices need to transmit their features in the first transmission. For notational simplicity, we define the attention vectors as  $\mathbf{a}_\tau := \{a_{k,\tau}\}_{k=1}^K$ ,  $\tau \in \{1, \dots, T\}$ . As illustrated in Fig. 3b, if the attention score  $a_{k,\tau}$  is 1, the feature  $\mathbf{u}_{k,\tau}$  would be transmitted from the edge device  $k$  to the edge server; Otherwise, the edge device  $k$  would be deactivated in the  $\tau$ -th transmission. In other words, we have  $\tilde{\mathbf{u}}_{k,\tau} = a_{k,\tau} \mathbf{u}_{k,\tau}$ .

### B. VDDIB-SR Objective

By adopting the stopping policy and introducing the attention module, we extend the VDDIB objective in (16) to the VDDIB-SR objective as follows:

$$\begin{aligned} \mathcal{L}_{\text{VDDIB-SR}} \left( \beta, T; \tilde{\phi}, \tilde{\psi}, \{\psi_k\}_{k=1}^K \right) := & \mathbf{E}_{p_\theta(z_{1:K}, \mathbf{y})} \left\{ \frac{1}{T} \sum_{\tau=1}^T -\log p_{\tilde{\psi}_\tau}(\mathbf{y} | \{\tilde{\mathbf{u}}_{1:K,t}\}_{t=1}^\tau) \right. \\ & \left. + \beta \left\{ \sum_{k=1}^K -\log p_{\psi_k}(\mathbf{y} | \mathbf{u}_k) + \sum_{k=1}^K \sum_{t=1}^T R_{\text{bit}}(\tilde{\mathbf{u}}_{k,t}) \right\} \right\}. \end{aligned} \quad (25)$$

In (25), the total loss of the internal predictors is shown in the first term that takes into account all possible stopping points. The second term in the VDDIB-SR objective acts as an auxiliary loss, which maintains the informativeness of each encoded feature and makes the training process robust against dynamic activation caused by the attention module. Besides, each  $R_{\text{bit}}(\tilde{\mathbf{u}}_{k,t}) = a_{k,t} n_k d_k$  in the third term of the VDDIB-SR objective measures the communication overhead at the  $t$ -th transmission of the edge device  $k$ .

By applying the Monte Carlo sampling method, we obtain an unbiased estimate of the gradient and hence minimize the objective in (25) using backpropagation. Given a minibatch of data  $\{\mathbf{x}_{1:K}^m, \mathbf{y}^m\}_{m=1}^M$ , we can extract the task-relevant features  $\{z_{1:K}^m\}_{m=1}^M$  by the learned parameters  $\{\theta_k\}_{k=1}^K$  in the VIB framework. The Monte Carlo estimate of  $\mathcal{L}_{\text{VDDIB-SR}}$  is given as follows:

$$\begin{aligned} \mathcal{L}_{\text{VDDIB-SR}} \left( \beta, T; \tilde{\phi}, \tilde{\psi}, \{\psi_k\}_{k=1}^K \right) \simeq & \frac{1}{M} \left\{ \frac{1}{T} \sum_{\tau=1}^T -\log p_{\tilde{\psi}_\tau}(\mathbf{y}^m | \{\tilde{\mathbf{u}}_{1:K,t}^m\}_{t=1}^\tau) \right. \\ & \left. + \beta \sum_{k=1}^K \left\{ -\log p_{\psi_k}(\mathbf{y}^m | \mathbf{u}_k^m) + \sum_{t=1}^T R_{\text{bit}}(\tilde{\mathbf{u}}_{k,t}^m) \right\} \right\}. \end{aligned} \quad (26)$$

---

**Algorithm 3** Training Procedures for the VDDIB-SR Method
 

---

**Input:** Training dataset  $\mathcal{D}$ , batch size  $M$ , optimized parameters  $\{\theta_k\}_{k=1}^K$ , and initialized parameters  $\tilde{\phi}$ ,  $\tilde{\psi}$ , and  $\{\psi_k\}_{k=1}^K$ .

**Output:** The optimized parameters  $\tilde{\phi}$ ,  $\tilde{\psi}$ , and  $\{\psi_k\}_{k=1}^K$ .

- 1: **repeat**
- 2: Randomly select a minibatch of data  $\{(\mathbf{x}_{1:K}^m, \mathbf{y}^m)\}_{m=1}^M$  from  $\mathcal{D}$ .
- 3: Extract the task-relevant features  $\{\mathbf{z}_{1:K}^m\}_{m=1}^M$  based on the learned distributions  $\{p_{\theta_k}(\mathbf{z}_k|\mathbf{x}_k)\}_{k=1}^K$ .
- 4: **while**  $\tau = 2$  to  $T$  **do**
- 5:     Compute the attention scores  $a_{k,\tau}$  for  $k \in 1 : K$  based on (24).
- 6:     Determine the transmitted features  $\tilde{\mathbf{u}}_{k,\tau} := a_{k,\tau} \mathbf{u}_{k,\tau}$  for  $k \in 1 : K$ .
- 7:     Obtain the intermediate inference result based on (21).
- 8: **end while**
- 9:     Compute the loss  $\mathcal{L}_{\text{VDDIB-SR}}(\beta, T; \tilde{\phi}, \tilde{\psi}, \{\psi_k\}_{k=1}^K)$  based on (26).
- 10:     Update parameters  $\tilde{\phi}$ ,  $\tilde{\psi}$ , and  $\{\psi_k\}_{k=1}^K$  through backpropagation.
- 11: **until** Convergence of parameters  $\tilde{\phi}$ ,  $\tilde{\psi}$ , and  $\{\psi_k\}_{k=1}^K$ .

---

The training procedures for the VDDIB-SR method are summarized in Algorithm 3.

**Remark 2.** *In contrast to the VDDIB method, the VDDIB-SR objective is no longer an upper bound of the DIB objective in (9). However, it satisfies the following property:*

$$\min_{\{p(\mathbf{u}_k|\mathbf{z}_k)\}_{k=1}^K} \mathcal{L}_{\text{DIB}}(\beta) - \min_{\tilde{\phi}, \tilde{\psi}, \{\psi_k\}_{k=1}^K} \mathcal{L}_{\text{VDDIB-SR}}(\beta, T; \tilde{\phi}, \tilde{\psi}, \{\psi_k\}_{k=1}^K) \leq \mathcal{C}(\beta, \mathbf{P}_T), \quad (27)$$

where function  $\mathcal{C}(\beta, \mathbf{P}_T)$  and the set of conditional distributions  $\mathbf{P}_T$  representing the distributed feature encoding schemes are defined as follows:

$$\mathcal{C}(\beta, \mathbf{P}_T) := \min_{\mathbf{P}_1} \mathcal{L}_{\text{DIB}}(\beta) - \min_{\mathbf{P}_T} \mathcal{L}_{\text{DIB}}(\beta), \quad (28)$$

$$\mathbf{P}_T := \left\{ p(\mathbf{u}_{k,1}|\mathbf{z}_k), p(\mathbf{u}_{k,2}|\mathbf{z}_k, \mathbf{u}_{1:K,1}), \dots, p(\mathbf{u}_{k,T}|\mathbf{z}_k, \{\mathbf{u}_{1:K,t}\}_{t=1}^{T-1}) \right\}_{k=1}^K. \quad (29)$$

It is straightforward that  $\mathbf{P}_1 \subseteq \dots \subseteq \mathbf{P}_T$ . Thus,  $\mathcal{C}(\beta, \mathbf{P}_T)$  is non-negative, which implies that the minimum of the VDDIB-SR objective is smaller than that of the VDDIB objective since the VDDIB objective is upper bounded by the DIB objective as shown in (20). Besides,  $\mathcal{C}(\beta, \mathbf{P}_T)$  increases with the integer  $T$ , which means that increasing the maximum transmission attempts  $T$  could achieve a better rate-relevance tradeoff. Let  $\mathbf{P} = \{p(\mathbf{u}_{1:K}|\mathbf{z}_{1:K})\}$  denote the family of joint feature encoding schemes. Function  $\mathcal{C}(\beta, \mathbf{P}_T)$  is lower bounded by  $\mathcal{C}(\beta, \mathbf{P})$  for any integer  $T$  as  $\mathbf{P}_T \subseteq \mathbf{P}$ . This is consistent with the classic source coding theory [28] that the performance

of the joint coding schemes is better than that of the distributed coding methods. The detailed derivation is deferred to Appendix C.

## VI. PERFORMANCE EVALUATION

In this section, we evaluate the performance of the proposed methods on two cooperative inference tasks, including a multi-view image classification task and a multi-view shape recognition task.

### A. Experimental Setup

1) *Datasets*: We use the MNIST dataset [35] for multi-view image classification, which consists of  $28 \times 28$  handwritten digit images in 10 classes. Each class has 6,000 samples for training and 1,000 samples for testing. We vertically split each image to two views and assume that there are two devices with distinct views in the edge inference system. Besides, we select the ModelNet40 dataset [36] for the multi-view shape recognition task, which contains 12,311 computer-aided design (CAD) shapes of 40 categories. Each shape is augmented by rotating 30 degrees along the gravity direction, resulting in twelve views. Similar to a prior study [26], we choose around 80 shapes per class for training and 20 shapes per class for testing.

2) *Proposed methods*: We investigate the performance of the proposed VDDIB and VDDIB-SR methods. The VDDIB-SR method with  $t$  transmissions is denoted as VDDIB-SR ( $T=t$ ). Particularly, the VDDIB method can be regarded as a special case of the VDDIB-SR method with  $T = 1$ . In the training process, we set  $\gamma = 10^{-4}$  when minimizing the VIB objective  $\mathcal{L}_{\text{VIB},k}(\gamma)$  for feature extraction. To achieve different rate-relevance tuples, the hyperparameter  $\beta$  varies in the range of  $[10^{-3}, 10^{-1}]$  when optimizing the VDDIB and VDDIB-SR objectives<sup>2</sup>.

3) *Baselines*: There are only a few existing studies that are relevant to feature encoding for cooperative edge inference. We compare the proposed methods against the following five baseline methods:

- *Server-based inference*: This baseline deploys a powerful DNN on the edge server for inference and adopts the data-oriented communication scheme to transmit the multiple views from the edge devices to the edge server.

<sup>2</sup>The code is coming soon.

- NN-REG and NN-GBI [23]: Both of them adopt learning-based methods to quantize the input data to bitstreams at the edge device. The DNN-based quantizers are either trained using the quantization loss regularization (NN-REG) or with the greedy boundary insertion (GBI) algorithm (NN-GBI).
- eSAFS [24]: In this scheme, each edge device extracts a feature vector as well as a small-scale importance vector using DNNs. These importance vectors are transmitted to an edge server for preprocessing, which identifies the important feature vectors that need to be transmitted by the edge devices.
- CAFS [25]: The method integrates a context-aware feature selection (CAFS) scheme into the multi-device cooperative edge inference system. Each edge device extracts a task-relevant feature and determines its importance via entropy-based likelihood estimation. The features from different devices are aggregated using a weighted mean of their likelihoods. By regulating the likelihood cut-off level, edge devices with less important features are deactivated.

4) *Neural Network Architecture*: In the edge inference system, each raw input sample is passed through the first part of the network (denoted as  $NN_1$ ) to extract the view-specific features, and the multiple features are collected for the processing of the remaining part of the network (denoted as  $NN_2$ ) to output the inference result. In the multi-view image classification task,  $NN_1$  is constructed by a 2-layer multi-layer perceptron (MLP), and  $NN_2$  consists of a 1-layer MLP; For multi-view shape recognition, we adopt the multi-view convolutional neural network (MVCNN) presented in [26] as the backbone, where  $NN_1$  adopts the convolutional layers in VGG-11 [37] for feature extraction, and  $NN_2$  consists of three fully-connected layers to predict the inference results.

The architectures of different methods are presented in Table I, where most of the methods adopt a uniform quantizer to discretize the output of  $NN_1$  for efficient transmission. In particular, the NN-GBI method adopts the GBI algorithm [23] to design a non-uniform quantizer, and the server-based inference scheme transmits the raw input views to the edge server via data-oriented communication. After receiving the extracted features, the NN-REG, NN-GBI, and VDDIB methods use vector concatenation for feature aggregation. The CAFS method leverages a weighted pooling layer to fuse the received features, where the weights are determined by the likelihood estimation module [25]. Besides, the eSAFS method performs signification-aware feature selection [4] to identify the most informative feature maps for transmission. Our proposed

TABLE I: The neural network architectures of different methods.

	Server-based Inference	NN-REG	NN-GBI	eSAFS	CAFS	VDDIB	VDDIB-SR
On-device Network	—	NN <sub>1</sub>	NN <sub>1</sub>	NN <sub>1</sub>	NN <sub>1</sub> Likelihood Estimation [25]	NN <sub>1</sub>	NN <sub>1</sub>
		Uniform Quantizer	GBI-based Quantizer [23]	Uniform Quantizer	Uniform Quantizer	Uniform Quantizer	Uniform Quantizer
Server-based Network	NN <sub>1</sub>	Feature Vector Concatenation	Feature Vector Concatenation	Significant-Aware Feature Selection [4]	Weighted Pooling Layer	Feature Vector Concatenation	Selective Retransmission
	NN <sub>2</sub>	NN <sub>2</sub>	NN <sub>2</sub>	NN <sub>2</sub>	NN <sub>2</sub>	NN <sub>2</sub>	NN <sub>2</sub>

VDDIB-SR leverages a selective retransmission mechanism to collect the features, where the attention module adopts two fully-connected layers to output the attention scores.

5) *Metrics*: We investigate the rate-relevance tradeoff of different multi-device edge inference schemes, where the rate is measured by the total number of bits ( $R_{\text{sum}}$ ) to be transmitted from the edge devices to the edge server, and the relevance is measured by the classification accuracy. In particular, we neglect the feedback signaling cost in the VDDIB-SR and eSAFS [24] methods due to the much lower communication overhead compared with that of the forward transmission, as well as the abundant radio resources for the downlink transmission. In the training process, we use the cross-entropy loss to measure the difference between the predicted results and the ground truths. Besides, the proposed VDDIB-SR method selects the maximum predicted probability in (23) as the confidence score.

### B. Multi-View Image Classification

This task aims to classify each image to its digit value from two distinct views. We compare the inference performance given different constraints on the average received bits  $R_{\text{sum}}$  over the test set. Table II shows the classification accuracy under different bit constraints, where the proposed VDDIB method achieves a comparable or better accuracy compared with the baselines, and the performance gain is more prominent when the communication overhead is smaller. This implies the effectiveness of the IB and DIB frameworks for task-oriented communication in multi-device edge inference systems. Besides, the accuracy achieved by the VDDIB-SR method is higher than that of the VDDIB method. This is attributed to the selective retransmission mechanism that eliminates the redundancy among the encoded features. Compared with the

TABLE II: The accuracy of the multi-view image classification task under different bit constraints. The server-based inference method achieves an accuracy of around 98.6% with 1.3 kbits overhead via data-oriented communication.

	$R_{\text{sum}}$		
	6 bits	10 bits	14 bits
NN-REG	95.93%	97.49%	97.78%
NN-GBI	96.62%	97.79%	98.02%
eSAFS	96.97%	97.87%	98.05%
CAFS	94.14%	97.43%	97.42%
VDDIB (ours)	97.08%	97.82%	98.06%
VDDIB-SR (T=2) (ours)	<b>97.13%</b>	<b>98.13%</b>	<b>98.22%</b>

TABLE III: The accuracy of the multi-view shape recognition task under different bit constraints. The server-based inference method achieves an accuracy of around 92% with 120 KB overhead via data-oriented communication.

	$R_{\text{sum}}$		
	120 bits	240 bits	360 bits
NN-REG	87.50%	88.25%	89.03%
NN-GBI*	88.82%	—	—
eSAFS	85.88%	87.87%	89.50%
CAFS	86.75%	89.56%	90.67%
VDDIB (ours)	89.25%	90.03%	90.75%
VDDIB-SR (T=2) (ours)	<b>90.25%</b>	<b>91.31%</b>	<b>91.62%</b>

\* The GBI quantization algorithm is computationally prohibitive when the number of bits is too large.

server-based inference scheme that achieves an accuracy of around 98.58% and induces 1.3 kbits overhead via data-oriented communication, our proposed VDDIB-SR method reduces the communication overhead by 98.8% with marginal performance degradation.

### C. Multi-View Shape Recognition

This task aims to recognize the 3D object based on a collection of perceived 2D views. Consider that there are twelve devices with distinct views in the multi-device cooperative edge inference system. We compare the inference performance given different rate constraints. Table

III summarizes the inference accuracy for the multi-view shape recognition task. We see that our methods consistently outperform the baselines under all rate constraints. This is because the proposed communication schemes are capable of discarding the task-irrelevant information. Besides, with the selective retransmission mechanism, the VDDIB-SR method secures further performance enhancement compared with the VDDIB method. The server-based inference method that offloads raw input views to the edge server by data-oriented communication achieves an accuracy of around 92%. However, it induces around 120 KB communication overhead, leading to intolerable latency. Specifically, if the multi-device cooperative inference system is supported by the narrowband Internet of Things (NB-IoT) standard with 18 KB/s uplink rate [38], the data-oriented communication scheme has a communication latency of 560 ms, while the proposed VDDIB-SR method largely reduces the latency to 2.5 ms and maintains comparable classification accuracy.

#### D. Ablation Study

1) *Impact of the maximum transmission attempts  $T$* : We investigate the performance of the VDDIB-SR method with different values of  $T$  on the multi-view image classification task. In particular, we adopt a joint coding scheme as a baseline method for comparison, which assumes that one edge device can access all the extracted view-specific features and perform joint feature encoding before transmission. The relationship between the achieved classification accuracy and the number of transmitted bits is shown in Fig. 4. It can be observed that the performance of the VDDIB-SR method improves with  $T$ , while the joint source coding scheme achieves the best performance and upper bound the VDDIB-SR method. These results are consistent with the analysis in Remark 2 that increasing the maximum transmission attempts  $T$  could achieve a better rate-relevance tradeoff<sup>3</sup>, and the joint coding scheme outperforms the distributed coding methods.

2) *Impact of the attention module*: To evaluate the performance of the attention module on communication overhead reduction, we select a baseline method denoted as VDDIB-Cascade for comparison, which removes the attention module from the VDDIB-SR method. We investigate

<sup>3</sup>Note that when  $T$  is sufficiently large, the feedback signaling cost is not neglectable. Selecting an optimal  $T$  that reduces the overall communication costs while maintaining the inference performance requires a dedicated communication protocol to manage the data flow, which is an interesting problem for future research. However, this problem is out of the scope of this paper.

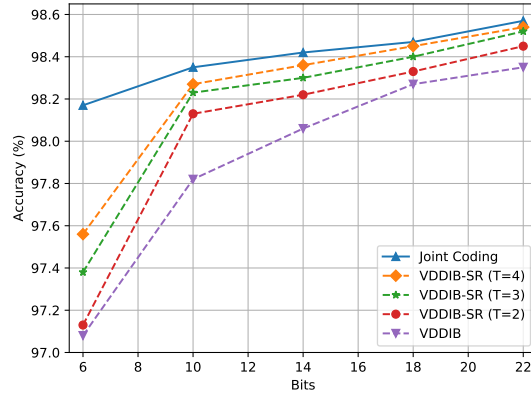


Fig. 4: Impact of the maximum transmission attempts  $T$  on the rate-relevance tradeoff.

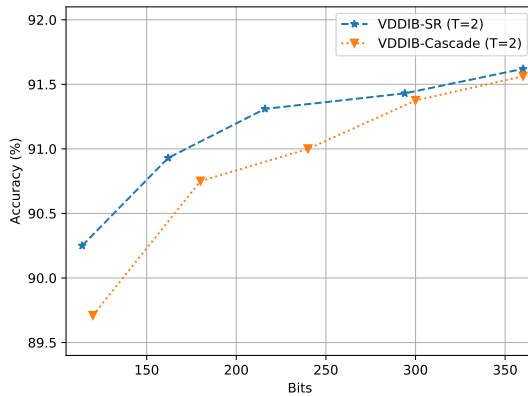


Fig. 5: Impact of the attention module on the rate-relevance tradeoff.

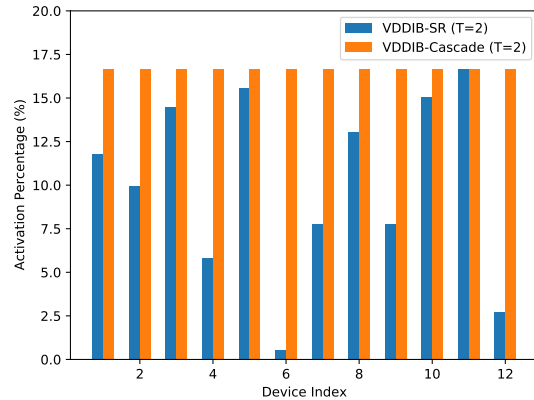


Fig. 6: The activation percentages of the edge devices in the retransmission.

the performance of these two methods on the multi-view shape recognition task. Specifically, the transmission attempt  $T$  is set to 2. As shown in Fig. 5, the VDDIB-SR method achieves a better rate-relevance tradeoff compared with the VDDIB-Cascade method, which demonstrates the effectiveness of the attention module. In particular, Fig. 6 depicts the activation percentages of the edge devices in the retransmission, where the VDDIB-SR and VDDIB-Cascade methods induce 216 bits and 240 bits overhead, respectively. Both methods achieve an accuracy of around 91.1%, and the communication cost reduction is attributed to the attention module that can schedule the edge devices with the most informative features to retransmit.

## VII. CONCLUSIONS

This work investigated task-oriented communication for multi-device cooperative edge inference, where a group of low-end edge devices transmit the task-relevant features to an edge server for aggregation and processing. Our proposed methods are built upon the IB principle and the DIB framework for feature extraction and distributed feature encoding, respectively. Compared with traditional data-oriented communication, our methods substantially reduce the communication overhead, thus enabling low-latency cooperative inference. Compared with existing methods for feature encoding in cooperative inference, we provide a theoretical framework to characterize the rate-relevance tradeoff, supported by pragmatic approaches for local feature extraction and distributed feature encoding, which consistently outperform baseline methods.

This study demonstrated the effectiveness of task-oriented communication for multi-device cooperative edge inference, which serves for the downstream task rather than for data reconstruction. The shifted objective of the communication system calls for new design tools. The IB-based frameworks, variational approximations, and retransmission mechanisms are promising candidates. Given the above, it is interesting to further investigate task-oriented communication strategies for other edge AI systems and applications, e.g., to design tighter bounds in variational approximations, to develop effective coding schemes for dynamic conditions, and to apply the IB-based methods to decentralized systems, etc.

### APPENDIX A

#### PROOF OF PROPOSITION 1

The proof of Proposition 1 relies on the following lemmas. We first prove that the extracted features  $(Z_1, \dots, Z_K)$  that satisfy the minimality condition in (2) are conditionally independent given  $Y$ .

**Lemma 1.** *For any joint distribution  $p(\mathbf{x}_{1:K}, \mathbf{y})$ , there exists a random variable  $Q$  that is independent of  $Y$  and satisfies  $p(\mathbf{x}_{1:K}, \mathbf{y}, \mathbf{q}) = p(\mathbf{y})p(\mathbf{q}) \prod_{k=1}^K p(\mathbf{x}_k | \mathbf{y}, \mathbf{q})$ .*

*Proof.* A trivial solution that satisfies  $p(\mathbf{x}_{1:K}, \mathbf{y}, \mathbf{q}) = p(\mathbf{y})p(\mathbf{q}) \prod_{k=1}^K p(\mathbf{x}_k | \mathbf{y}, \mathbf{q})$  is that  $p(\mathbf{q}) = p(\mathbf{x}_{1:K} | \mathbf{y})$ . □

Particularly, the random variables  $Y, Q, X_k, Z_k$  constitute the following Markov chain since the extracted feature  $Z_k$  is independent of  $(Y, Q)$  given the local data  $X_k$ :

$$(Y, Q) \leftrightarrow X_k \leftrightarrow Z_k, k \in \{1, \dots, K\}. \quad (30)$$

With the data processing inequality, we have  $I(Y, Q; Z_k) \leq I(X_k, Z_k)$ . Suppose the extracted features satisfy the minimality in (2), which implies  $I(X_k; Z_k) = I(Y; Z_k)$ ,  $k \in \{1, \dots, K\}$ . By incorporating the chain rule of mutual information, i.e.,  $I(Y; Z_k) \leq I(Y, Q; Z_k)$ , we get  $I(Y, Q; Z_k) = I(Y; Z_k)$ , which shows that the random variables  $Q, Y, Z_k$  constitute the Markov chain as follows:

$$Q \leftrightarrow Y \leftrightarrow Z_k, k \in \{1, \dots, K\}. \quad (31)$$

As each extracted feature  $z_k$  only depends on the corresponding observation  $x_k$ , the conditional distribution of  $(X_{1:K}, Z_{1:K})$  given  $(Y, Q)$  is as follows:

$$p(\mathbf{x}_{1:K}, \mathbf{z}_{1:K} | \mathbf{y}, \mathbf{q}) = \prod_{k=1}^K p(\mathbf{x}_k | \mathbf{y}, \mathbf{q}) p(\mathbf{z}_k | \mathbf{x}_k), \quad (32)$$

$$= \prod_{k=1}^K p(\mathbf{x}_k, \mathbf{z}_k | \mathbf{y}, \mathbf{q}). \quad (33)$$

where (32) is due to Lemma 1, and (33) is derived from the Markov chains in (30). By integrating out  $\mathbf{x}_{1:K}$  in (33), the conditional distribution of  $Z_{1:K}$  given  $(Y, Q)$  is as follows:

$$p(\mathbf{z}_{1:K} | \mathbf{y}, \mathbf{q}) = \prod_{k=1}^K p(\mathbf{z}_k | \mathbf{y}, \mathbf{q}), \quad (34)$$

$$= \prod_{k=1}^K p(\mathbf{z}_k | \mathbf{y}), \quad (35)$$

where (35) is due to the Markov chains in (31). By integrating out  $\mathbf{q}$  in the left-hand side of (35), we have  $p(\mathbf{z}_{1:K} | \mathbf{y}) = \prod_{k=1}^K p(\mathbf{z}_k | \mathbf{y})$ , which means that the features  $Z_{1:K}$  are conditionally independent given the target variable  $Y$ . With this property, we can leverage the following lemma to describe the rate-relevance region.

**Lemma 2.** *With the conditional independence  $p(\mathbf{z}_{1:K} | \mathbf{y}) = \prod_{k=1}^K p(\mathbf{z}_k | \mathbf{y})$ , the optimal rate-relevance tuples  $(\Delta, R_{\text{sum}})$  satisfy  $\Delta = \Delta(R_{\text{sum}})$ , where  $\Delta(R_{\text{sum}})$  represents the maximum relevance given the rate constraint  $R_{\text{sum}}$  defined as follows:*

$$\Delta(R_{\text{sum}}) := \max_{\{p(\mathbf{u}_k | \mathbf{z}_k)\}_{k=1}^K} \min \left\{ I(Y; U_{1:K}), R_{\text{sum}} - \sum_{k=1}^K I(Z_k; U_k | Y) \right\}. \quad (36)$$

For each optimal rate-relevance tuples  $(\Delta, R_{\text{sum}})$ , there exists  $\beta \geq 0$  such that  $(\Delta, R_{\text{sum}}) = (\Delta_\beta, R_\beta)$ , where

$$\Delta_\beta = I(Y; U_{1:K}^*), \quad (37)$$

$$R_\beta = \Delta_\beta + \sum_{k=1}^K [I(Z_k; U_k^*) - I(Y; U_k^*)], \quad (38)$$

and the encoded features  $U_{1:K}^*$  are obtained by minimizing the DIB objective in (9).

*Proof.* Please refer to the proof of Proposition 2 in [16]. □

By combining Lemma 1 and Lemma 2, we get Proposition 1. □

## APPENDIX B

### DERIVATION OF THE VARIATIONAL UPPER BOUND

#### A. Variational Information Bottleneck

Recall that the IB objective in (12) has the form  $\mathcal{L}_{\text{IB},k}(\gamma) = H(Y|Z_k) + \gamma I(X_k; Z_k)$  at device  $k \in \{1, \dots, K\}$ . Writing it out in full with the conditional distribution  $p_{\theta_k}(\mathbf{z}_k|\mathbf{x})$  and the variational distributions  $p_{\varphi_k}(\mathbf{y}|\mathbf{z}_k)$ ,  $r_k(\mathbf{z}_k)$ , it becomes:

$$\begin{aligned} \mathcal{L}_{\text{IB},k}(\gamma) &= \mathbf{E}_{p(\mathbf{x}_k, \mathbf{y})} \left\{ \mathbf{E}_{p_{\theta_k}(\mathbf{z}_k|\mathbf{x}_k)} [-\log p(\mathbf{y}|\mathbf{z}_k)] + \gamma D_{\text{KL}}(p(\mathbf{z}_k|\mathbf{x}_k) \| p(\mathbf{z}_k)) \right\}, \\ &= \underbrace{\mathbf{E}_{p(\mathbf{x}_k, \mathbf{y})} \left\{ \mathbf{E}_{p_{\theta_k}(\mathbf{z}_k|\mathbf{x}_k)} [-\log p_{\varphi_k}(\mathbf{y}|\mathbf{z}_k)] + \gamma D_{\text{KL}}(p(\mathbf{z}_k|\mathbf{x}_k) \| p(\mathbf{z}_k)) \right\}}_{\mathcal{L}_{\text{VIB},k}(\gamma; \theta_k, \varphi_k)} \\ &\quad - \mathbf{E}_{p(\mathbf{x}_k, \mathbf{y})} \left\{ D_{\text{KL}}(p(\mathbf{y}|\mathbf{z}_k) \| p_{\varphi_k}(\mathbf{y}|\mathbf{z}_k)) + \gamma D_{\text{KL}}(p(\mathbf{z}_k) \| r_k(\mathbf{z}_k)) \right\}. \end{aligned}$$

$\mathcal{L}_{\text{VIB},k}(\gamma; \theta_k, \varphi_k)$  in the above equation is the VIB objective function in (12). As the KL-divergence is non-negative, the VIB objective function is an upper bound of the IB objective function.

#### B. Variational Distributed Deterministic Information Bottleneck

Revisit the DDIB objective function  $\mathcal{L}_{\text{DDIB}}(\beta) = H(Y|U_{1:K}) + \beta \sum_{k=1}^K [H(Y|U_k) + R_{\text{bit}}(U_k)]$  in (15). Writing it out with the learned distribution  $p_{\theta}(\mathbf{z}_{1:K}, \mathbf{y})$  and the encoding functions

$\mathbf{u}_k = \mathcal{Q}_k(\mathbf{f}_{\phi_k}(\mathbf{z}_k))$ ,  $k \in \{1, \dots, K\}$ , we have:

$$\begin{aligned} \mathcal{L}_{\text{DDIB}}(\beta) &= \mathbf{E}_{p_{\theta}(\mathbf{z}_{1:K}, \mathbf{y})} \left\{ -\log p(\mathbf{y}|\mathbf{u}_{1:K}) + \beta \sum_{k=1}^K [-\log p(\mathbf{y}|\mathbf{u}_k) + R_{\text{bit}}(\mathbf{u}_k)] \right\}, \\ &= \underbrace{\mathbf{E}_{p_{\theta}(\mathbf{z}_{1:K}, \mathbf{y})} \left\{ -\log p_{\psi_0}(\mathbf{y}|\mathbf{u}_{1:K}) + \beta \sum_{k=1}^K [-\log p_{\psi_k}(\mathbf{y}|\mathbf{u}_k) + R_{\text{bit}}(\mathbf{u}_k)] \right\}}_{\mathcal{L}_{\text{VDDIB}}(\beta; \phi, \psi)} \\ &\quad - \mathbf{E}_{p_{\theta}(\mathbf{z}_{1:K}, \mathbf{y})} \left\{ D_{\text{KL}}(p(\mathbf{y}|\mathbf{u}_{1:K}) \| p_{\psi_0}(\mathbf{y}|\mathbf{u}_{1:K})) + \beta \sum_{k=1}^K D_{\text{KL}}(p(\mathbf{y}|\mathbf{u}_k) \| p_{\psi_k}(\mathbf{y}|\mathbf{u}_k)) \right\}. \end{aligned}$$

As the KL-divergence is non-negative, the VDDIB objective function is a variational upper bound of the DDIB objective function.

## APPENDIX C

### DERIVATION OF REMARK 2

In this part, we aim to detail the derivation of the inequality in (27). Based on the definition in (28), it is equivalent to validate the following inequality to show (27):

$$\min_{\tilde{\phi}, \tilde{\psi}, \{\psi_k\}_{k=1}^K} \mathcal{L}_{\text{VDDIB-SR}}(\beta, T; \tilde{\phi}, \tilde{\psi}, \{\psi_k\}_{k=1}^K) \geq \min_{\mathbf{P}_T} \mathcal{L}_{\text{DIB}}(\beta). \quad (39)$$

Revisit the DIB objective  $\mathcal{L}_{\text{DIB}}(\beta) = H(Y|U_{1:K}) + \beta \sum_{k=1}^K [H(Y|U_k) + I(Z_k; U_k)]$  in (9). It satisfies the following inequality:

$$\begin{aligned} \mathcal{L}_{\text{DIB}}(\beta) &\leq \mathbf{E}_{p_{\theta}(\mathbf{z}_{1:K}, \mathbf{y})} \left\{ \mathbf{E}_{p(\mathbf{u}_{1:K}|\mathbf{z}_{1:K})} \left\{ -\log p(\mathbf{y}|\mathbf{u}_{1:K}) \right. \right. \\ &\quad \left. \left. + \beta \sum_{k=1}^K \left[ -\log p(\mathbf{y}|\mathbf{u}_k) + \sum_{t=1}^T R_{\text{bit}}(\mathbf{u}_{k,t}) \right] \right\} \right\}, \quad (40) \end{aligned}$$

$$\begin{aligned} &\leq \mathbf{E}_{p_{\theta}(\mathbf{z}_{1:K}, \mathbf{y})} \left\{ \mathbf{E}_{p(\mathbf{u}_{1:K}|\mathbf{z}_{1:K})} \left\{ \sum_{\tau=1}^T -\log p_{\tilde{\psi}_{\tau}}(\mathbf{y}|\{\mathbf{u}_{1:K}, t\}_{t=1}^{\tau}) \right. \right. \\ &\quad \left. \left. + \beta \sum_{k=1}^K \left[ -\log p_{\psi_k}(\mathbf{y}|\mathbf{u}_k) + \sum_{t=1}^T R_{\text{bit}}(\mathbf{u}_{k,t}) \right] \right\} \right\}, \quad (41) \end{aligned}$$

where (40) follows the inequalities  $I(Z_k; U_k) \leq \sum_{t=1}^T H(U_{k,t})$  and  $H(U_{k,t}) \leq R_{\text{bit}}(U_{k,t})$ , and (41) is due to the chain rule of conditional entropy and the variational approximations. Denoting the right-hand side of (41) as  $\mathcal{L}(T; \tilde{\psi}, \{\psi_k\}_{k=1}^K)$ , it satisfies:

$$\min_{\tilde{\phi}, \tilde{\psi}, \{\psi_k\}_{k=1}^K} \mathcal{L}_{\text{VDDIB-SR}}(\beta, T; \tilde{\phi}, \tilde{\psi}, \{\psi_k\}_{k=1}^K) \geq \min_{\mathbf{P}_T, \tilde{\psi}, \{\psi_k\}_{k=1}^K} \mathcal{L}(T; \tilde{\psi}, \{\psi_k\}_{k=1}^K), \quad (42)$$

since the family of conditional distributions  $\{p(\mathbf{u}_{1:K}|\mathbf{z}_{1:K})\}$  parameterized by  $\tilde{\phi}$  is a subset of  $\mathcal{P}_T$ . By combining (41) and (42), we are able to show the inequality in (39).

## REFERENCES

- [1] C. Szegedy, V. Vanhoucke, S. Ioffe, J. Shlens, and Z. Wojna, “Rethinking the inception architecture for computer vision,” in *Proc. IEEE Conf. Comput. Vision Pattern Recognit.*, Las Vegas, NV, USA, Jun. 2016.
- [2] X. Hou, S. Dey, J. Zhang, and M. Budagavi, “Predictive view generation to enable mobile 360-degree and VR experiences,” in *Proc. Morning Workshop VR AR Netw.*, Budapest, Hungary, Aug. 2018.
- [3] R. Collobert and J. Weston, “A unified architecture for natural language processing: Deep neural networks with multitask learning,” in *Proc. Int. Conf. Mach. Learn.*, Helsinki, Finland, Jul. 2008.
- [4] Y. Shi, K. Yang, T. Jiang, J. Zhang, and K. B. Letaief, “Communication-efficient edge AI: Algorithms and systems,” *IEEE Commun. Surv. Tut.*, vol. 22, no. 4, pp. 2167–2191, Jul. 2020.
- [5] J. Shao and J. Zhang, “Communication-computation trade-off in resource-constrained edge inference,” *IEEE Commun. Mag.*, vol. 58, no. 12, pp. 20–26, Dec. 2020.
- [6] C. Badue, R. Guidolini, R. V. Carneiro, P. Azevedo, V. B. Cardoso, A. Forechi, L. Jesus, R. Berriel, T. M. Paixao, F. Mutz *et al.*, “Self-driving cars: A survey,” *Expert Syst. Appl.*, p. 113816, Mar. 2020.
- [7] E. Unlu, E. Zenou, N. Riviere, and P.-E. Dupouy, “Deep learning-based strategies for the detection and tracking of drones using several cameras,” *IPSA Trans. Comput. Vision Appl.*, vol. 11, no. 1, pp. 1–13, Jul. 2019.
- [8] D. Zou, P. Tan, and W. Yu, “Collaborative visual slam for multiple agents: A brief survey,” *Virtual Reality Intell. Hardware*, vol. 1, no. 5, pp. 461–482, Oct. 2019.
- [9] Z. Zhou, X. Chen, E. Li, L. Zeng, K. Luo, and J. Zhang, “Edge intelligence: Paving the last mile of artificial intelligence with edge computing,” *Proc. IEEE*, vol. 107, no. 8, pp. 1738–1762, Aug. 2019.
- [10] J. Shao and J. Zhang, “Bottlenet++: An end-to-end approach for feature compression in device-edge co-inference systems,” in *Proc. IEEE Int. Conf. Commun. Workshop*, Dublin, Ireland, Jun. 2020.
- [11] J. Shao, H. Zhang, Y. Mao, and J. Zhang, “Branchy-gnn: A device-edge co-inference framework for efficient point cloud processing,” in *Proc. IEEE Int. Conf. Acoust. Speech Signal Process. (ICASSP)*, Toronto, Canada, Jun. 2021.
- [12] J. Shao, Y. Mao, and J. Zhang, “Learning task-oriented communication for edge inference: An information bottleneck approach,” 2021. [Online]. Available: <https://arxiv.org/abs/2102.04170>.
- [13] X. Liu, W. Liu, T. Mei, and H. Ma, “A deep learning-based approach to progressive vehicle re-identification for urban surveillance,” in *Proc. Eur. Conf. Comput. Vision (ECCV)*, Amsterdam, Netherlands, Oct. 2016.
- [14] N. Tishby, F. C. Pereira, and W. Bialek, “The information bottleneck method,” in *Proc. Annu. Allerton Conf. Commun. Control Comput.*, Monticello, IL, USA, Oct. 2000.
- [15] T. A. Courtade and T. Weissman, “Multiterminal source coding under logarithmic loss,” *IEEE Trans. Inf. Theory*, vol. 60, no. 1, pp. 740–761, Nov. 2013.
- [16] I. E. Aguerri and A. Zaidi, “Distributed variational representation learning,” *IEEE Trans. Pattern Anal. Mach. Intell.*, vol. 43, no. 1, pp. 120–138, Jan. 2021.
- [17] E. C. Strinati and S. Barbarossa, “6g networks: Beyond shannon towards semantic and goal-oriented communications,” *Comput. Netw.*, vol. 190, p. 107930, May 2021.
- [18] G. Zhu, D. Liu, Y. Du, C. You, J. Zhang, and K. Huang, “Toward an intelligent edge: wireless communication meets machine learning,” *IEEE Commun. Mag.*, vol. 58, no. 1, pp. 19–25, Jan. 2020.

- [19] A. E. Eshratifar, A. Esmaili, and M. Pedram, "Bottleneck: A deep learning architecture for intelligent mobile cloud computing services," 2019. [Online]. Available: <https://arxiv.org/abs/1902.01000>.
- [20] Y. Dubois, B. Bloem-Reddy, K. Ullrich, and C. J. Maddison, "Lossy compression for lossless prediction," in *Proc. Int. Conf. Learn. Represent. Workshop on Neural Compression*, May 2021. [Online]. Available: <https://openreview.net/forum?id=GfCs5NhoR8Q>.
- [21] M. Jankowski, D. Gündüz, and K. Mikolajczyk, "Wireless image retrieval at the edge," *IEEE J. Sel. Areas Commun.*, vol. 39, no. 1, pp. 89–100, May 2021.
- [22] D. Slepian and J. Wolf, "Noiseless coding of correlated information sources," *IEEE Trans. Inf. Theory*, vol. 19, no. 4, pp. 471–480, Jul 1973.
- [23] O. A. Hanna, Y. H. Ezzeldin, T. Sadjadpour, C. Fragouli, and S. Diggavi, "On distributed quantization for classification," *IEEE J. Sel. Areas Inf. Theory*, vol. 1, no. 1, pp. 237–249, Apr. 2020.
- [24] M. Singhal, V. Raghunathan, and A. Raghunathan, "Communication-efficient view-pooling for distributed multi-view neural networks," in *Proc. Design Automat. Test Eur. Conf. Exhib. (DATE)*, Grenoble, France, Sep. 2020.
- [25] J. Choi, Z. Hakimi, P. W. Shin, J. Sampson, and V. Narayanan, "Context-aware convolutional neural network over distributed system in collaborative computing," in *Proc. ACM/IEEE Design Automat. Conf. (DAC)*, Las Vegas, NV, USA, Jun. 2019.
- [26] H. Su, S. Maji, E. Kalogerakis, and E. Learned-Miller, "Multi-view convolutional neural networks for 3d shape recognition," in *Proc. Int. Conf. Comput. Vision*, Santiago, Chile, Dec. 2015.
- [27] A. A. Alemi, I. Fischer, J. V. Dillon, and K. Murphy, "Deep variational information bottleneck," in *Proc. Int. Conf. Learn. Represent.*, Toulon, France, Apr. 2017.
- [28] A. El Gamal and Y.-H. Kim, *Network information theory*. Cambridge university press, 2011.
- [29] D. M. Blei, A. Kucukelbir, and J. D. McAuliffe, "Variational inference: A review for statisticians," *J. Amer. Statist. Assoc.*, vol. 112, no. 518, pp. 859–877, Jul. 2017.
- [30] D. P. Kingma and M. Welling, "Auto-encoding variational bayes," in *Proc. Int. Conf. Learn. Represent.*, Banff, Canada, Apr. 2014.
- [31] Z. Goldfeld and Y. Polyanskiy, "The information bottleneck problem and its applications in machine learning," *IEEE J. Sel. Areas Inf. Theory*, vol. 1, no. 1, pp. 19–38, Apr. 2020.
- [32] Y. Bengio, N. Léonard, and A. Courville, "Estimating or propagating gradients through stochastic neurons for conditional computation," *arXiv preprint arXiv:1308.3432*, 2013. [Online]. Available: <https://arxiv.org/abs/1308.3432>.
- [33] X. Chen, H. Dai, Y. Li, X. Gao, and L. Song, "Learning to stop while learning to predict," in *Int. Conf. Mach. Learn.*, Vienna, Australia, Apr. 2020.
- [34] S. Enomoto and T. Eda, "Learning to cascade: Confidence calibration for improving the accuracy and computational cost of cascade inference systems," in *Proc. AAAI Conf. Artif. Intell.*, Feb. 2021. [Online]. Available: <https://www.aaai.org/AAAI21Papers/AAAI-2189.EnomotoS.pdf>.
- [35] Y. Lecun, L. Bottou, Y. Bengio, and P. Haffner, "Gradient-based learning applied to document recognition," *Proc. IEEE*, vol. 86, no. 11, pp. 2278–2324, May 1998.
- [36] Z. Wu, S. Song, A. Khosla, F. Yu, L. Zhang, X. Tang, and J. Xiao, "3d shapenets: A deep representation for volumetric shapes," in *Proc. IEEE/CVF Conf. Comput. Vision Pattern Recognit. (CVPR)*, Boston, MA, USA, Jun. 2015.
- [37] K. Simonyan and A. Zisserman, "Very deep convolutional networks for large-scale image recognition," in *Int. Conf. Learn. Represent.*, 2015.
- [38] A. D. Zayas and P. Merino, "The 3GPP NB-IoT system architecture for the internet of things," in *Proc. IEEE Int. Conf. Commun. Workshop*, May 2017, pp. 277–282.